


Cite this: *RSC Adv.*, 2022, **12**, 21129

Received 5th April 2022
Accepted 8th July 2022

DOI: 10.1039/d2ra02185d

rsc.li/rsc-advances

A turn-on fluorescent probe with high selectivity for Hg^{2+} and its applications in living cells[†]

Bin Li, ^a Fuli Tian^{*b} and Yupeng Hua^a

A novel fluorescent probe L with a rhodamine B lactam structure modified with 3-methyl-2-thiophenecarboxaldehyde has been prepared based on the thiophilicity of Hg^{2+} . The probe L exhibits a unique response with an “off-on-type” mode towards Hg^{2+} among other biologically relevant metal cations. The limit of detection (LOD) for probe L is 1.5 ppb. In addition, in the presence of Hg^{2+} , the probe L shows a colorimetric response from colorless to pink. The recognition behavior of probe L towards Hg^{2+} has been investigated by ^1H NMR titration experiments, Job's plot, and MS and IR analyses. As a result, the ligation between the probe and Hg^{2+} leads to the scission of the spirolactam bond of free L and the restoration of its conjugated structure, which can give rise to the fluorescence enhancement of the probe L. Besides, it also can be used as a sensitivity probe in living cells for Hg^{2+} sensing, which can meet various needs in genetic and environmental samples.

Introduction

Mercury is one of the highly toxic heavy metal element for the environment and human health, which is generated by numerous sources such as coal plants, gold production, and mercury lamps.^{1–3} Because of the strong affinity for the thiol groups of proteins, Hg^{2+} has been linked to a number of neurological issues such as brain damage and kidney damage.^{4–8} Since Hg^{2+} ions are highly toxic and easily penetrate the blood–brain barrier, the EPA has set a limit of 2×10^{-9} M in drinking water⁹ in the U.S. Therefore, it is critical to find a reliable technique to detect and monitor small amounts of Hg^{2+} ions in genetic and environmental samples.

Numerous approaches have been applied to detect Hg^{2+} ions including atomic absorption spectroscopy, spectrophotometry, and voltammetry.^{10,11} These approaches provide respectable detection limits, whereas the majority of them involve the need for an advanced and expensive instrument as well as lengthy pretreatment operations, which are not suitable for real-time monitoring.¹² Fluorescence-based approaches have been gradually developed and become essential instruments in metal ion detection owing to their advantages of straightforward operation, high sensitivity and selectivity.^{13–15} The development of fluorescent indicators for Hg^{2+} ions has received considerable interest. There are a number of fluorescence probes for Hg^{2+} . However, some reported probes have several limitations such as

exhibited fluorescent “on-off” behavior owing to the intrinsic spectral property of Hg^{2+} ,^{16–18} solubility in organic solvents,¹⁹ non-colorimetric²⁰ and difficult synthesis.^{21–23} Therefore, the development of a colorimetric probe with a simple procedure, low detection limit, and “off-on” behavior in an aqueous solution is still necessary. The rhodamine B lactam with outstanding spectroscopic properties could be modified with 3-methyl-2-thiophenecarboxaldehyde based on the thiophilicity of Hg^{2+} . On the one hand, the probe is formed by the condensation of the aldehyde group with the amino group in the rhodamine lactam; on the other hand, the sulfur atom also potentially acts as a coordinating atom for Hg^{2+} . Therefore, it is expected that the synthesized probe L could be a potential coordinator for Hg^{2+} .

Herein, a new colorimetric probe (*E*-3',6'-bis(diethylamino)-2-(((3-methylthiophen-2-yl)methylene)amino)spiro[isoindoline-1,9'-xanthen]-3-one has been designed and synthesised. It shows a significant fluorescence behaviour and unique response for Hg^{2+} among other biologically relevant metal cations. In comparison with some reported probe of Hg^{2+} , the colorimetric probe L is easily synthesized, possessing low detection limits and “off-on” behavior in $\text{CH}_3\text{OH}-\text{H}_2\text{O}$ (4 : 1, v/v, Tris-HCl buffer pH = 8.0). Therefore, it has potential applications in various practical samples as a visible probe for Hg^{2+} .

Experimental

Materials

Hydrazine hydrate, 3-methyl-2-thiophenecarboxaldehyde and rhodamine B were used. All chemicals and solvents were purchased commercially. Stock solutions (1×10^{-5} M) of the probe were produced by dissolving 5.65 mg compounds L in the

^aDepartment of Chemical Engineering, Ordos Institute of Technology, Ordos 017000, PR China. E-mail: ftian@imu.edu.cn

^bCollege of Chemistry and Material Science, Hainan Vocational University of Science and Technology, Haikou 571126, P. R. China

† Electronic supplementary information (ESI) available. See <https://doi.org/10.1039/d2ra02185d>



mixed solvent ($\text{CH}_3\text{OH}-\text{H}_2\text{O} = 4:1$, v/v, pH = 8.0). Stock solutions (1.0×10^{-2} M) of Na^+ , Ag^+ , Al^{3+} , Ba^{2+} , Ca^{2+} , Cd^{2+} , Cr^{3+} , Cu^{2+} , Co^{2+} , Fe^{3+} , Hg^{2+} , K^+ , Mg^{2+} , Mn^{2+} , Ni^{2+} , Pb^{2+} , Sr^{2+} and Zn^{2+} were made by dissolving their nitrate salts in the above mixed solvent.

Instruments

^1H NMR and ^{13}C NMR signals were collected on a Bruker spectrometer using TMS as a standard. Absorption spectra were recorded on a U-3900 spectrophotometer at room temperature. Fluorescent emission was obtained using a Hitachi F-4600 spectrophotometer at room temperature. MS spectra were obtained on an Agilent 6546 Q-TOF LC/MS spectrometer. Fluorescence microscopy images were collected *via* laser scanning confocal microscopy. IR spectra were recorded in an anhydrous methanol solution using a Bruker TENSOR27.

Measurement

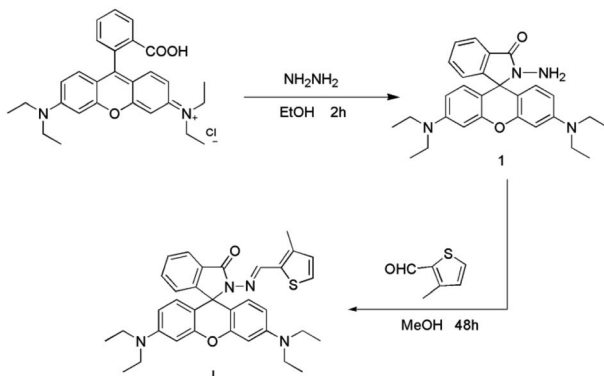
Test solutions were prepared by pouring 2 mL solution of **L** (10 μM) into the cuvettes with each metal ion stock solutions (20 μM , 10 mM). The prepared samples were shaken for 5 s at 25 °C. The excitation wavelength used for all fluorescence experiments was 490 nm.

Synthesis

The probe was successfully synthesized in two easy steps, as seen in Scheme 1.

Synthesis of compound 1. Compound **1** was synthesized by a previously reported.²⁴ It was prepared by refluxing rhodamine B (hydrochloride salt, 1.92 g, 4 mM) and excess hydrazine hydrate (85%, 5 mL) in 30 mL ethanol for 2 h at 25 °C. Pinkish solids (1.81 g) has been obtained. Yield: 95%. ^1H NMR (500 MHz, DMSO) δ 7.84–7.72 (m, 1H), 7.47 (dd, $J = 5.9, 3.2$ Hz, 2H), 6.99 (d, $J = 6.2$ Hz, 1H), 6.37 (s, 2H), 6.32 (d, $J = 8.8$ Hz, 4H), 4.28 (s, 2H), 3.32 (dd, $J = 13.8, 6.8$ Hz, 8H), 1.08 (t, $J = 6.9$ Hz, 12H) (Fig. S1†).

Synthesis of probe **L.** Compound **1** (1 mM) was dissolved in 30 mL absolute methanol, and then added 3-methyl-2-thiophenecarboxaldehyde (1 mM) under stirring condition. In the reaction system, 2–3 drops of acetic acid were added. A light



Scheme 1 Synthetic route to probe **L**.

pink precipitate was formed after refluxed 48 h at 80 °C. Filtered the precipitates were washed with ethanol three times, and pinkish solids (0.49 g, 86%) has been obtained. ^1H NMR (500 MHz, DMSO) δ 8.59 (s, 1H), 7.90 (d, $J = 7.3$ Hz, 1H), 7.58 (dt, $J = 21.4, 7.2$ Hz, 2H), 7.46 (d, $J = 4.9$ Hz, 1H), 7.08 (d, $J = 7.4$ Hz, 1H), 6.84 (d, $J = 4.9$ Hz, 1H), 6.43 (s, 2H), 6.39 (d, $J = 8.8$ Hz, 2H), 6.35 (dd, $J = 8.9, 1.6$ Hz, 2H), 3.32 (dd, $J = 14.4, 7.1$ Hz, 8H), 2.05 (s, 3H), 1.06 (t, $J = 6.9$ Hz, 12H) (Fig. S2†). ^{13}C NMR (126 MHz, DMSO) δ 163.87 (s), 152.98 (s), 149.02 (s), 140.42 (s), 134.33 (s), 133.31 (s), 131.28 (s), 129.25 (s), 129.06 (s), 128.57 (s), 128.28 (s), 124.26 (s), 123.35 (s), 108.70 (s), 105.28 (s), 97.59 (s), 65.44 (s), 44.16 (s), 13.61 (s), 12.82 (s) (Fig. S3†). MS(ESI): m/z [M + H]⁺: calcd for $\text{C}_{34}\text{H}_{36}\text{N}_4\text{O}_2\text{S}$: 565.26, found: 565.40 (Fig. S4†).

Result and discussion

Absorption and fluorescence selectivity of probe **L** towards Hg^{2+}

The absorption responses of probe **L** to various cations (Na^+ , Ag^+ , Al^{3+} , Ba^{2+} , Ca^{2+} , Cd^{2+} , Cr^{3+} , Cu^{2+} , Co^{2+} , Fe^{3+} , Hg^{2+} , K^+ , Mg^{2+} , Mn^{2+} , Ni^{2+} , Pb^{2+} , Sr^{2+} and Zn^{2+}) were examined. As shown in Fig. 1, the colorless probe **L** displayed weak absorptions at 251 nm and 315 nm, which belong to the thiophene group. In addition, only weak changes were observed when other cations were added. In the presence of Hg^{2+} ions, the peaks at 251 nm and 315 nm of receptor **L** significantly increased. Moreover, a new peak at 550 nm was discovered. Simultaneously, the color of the solution changed from colorless to pink. The new absorption band represents the scission of the spirolactam bond, and the restoring conjugated structure of probe **L**. These results indicated that probe **L** has a high selectivity to Hg^{2+} ions and could act as a colorimetric probe for Hg^{2+} .

In addition, the selectivity of probe **L** for Hg^{2+} ions was determined *via* fluorescence spectroscopy. As shown in Fig. 2, the free probe **L** exhibited a feeble fluorescence emission at 582 nm upon excitation at 490 nm. In comparison, the solution of probe **L** has a strong emission band in the presence of the Hg^{2+} ions at 582 nm but other cations did not cause any noticeable emission at 582 nm. These phenomena agree with

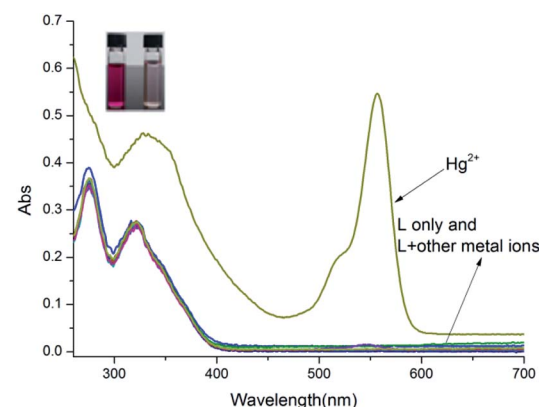


Fig. 1 The UV-vis absorption spectra changes of **L** (10 μM) in $\text{CH}_3\text{OH}-\text{H}_2\text{O}$ (4 : 1, v/v, Tris-HCl buffer pH = 8.0) upon being treated with 10 equiv. metal ions.



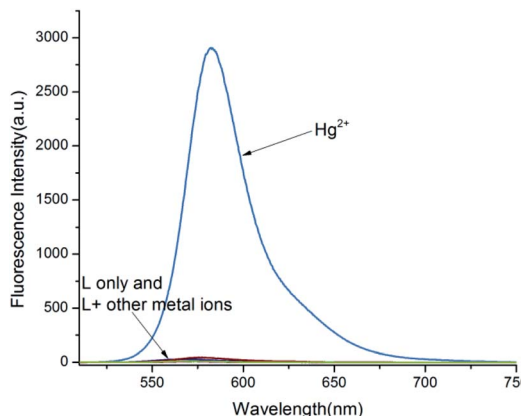


Fig. 2 Fluorescence responses of probe L upon treated with 10 equiv. metal ions in $\text{CH}_3\text{OH}-\text{H}_2\text{O}$ (4 : 1, v/v, Tris-HCl buffer pH = 8.0).

the results of the absorption spectrum, suggesting that probe **L** has a high sensitivity to Hg^{2+} because a complex was formed between **L** and Hg^{2+} ions.

Competition experiments

To study the selectivity of probe **L** towards Hg^{2+} over other biologically and environment-relevant cations, competitive experiments were conducted, as described in Fig. 3. The Hg^{2+} -induced emission of **L** was almost unaffected by other metal cations. These findings indicate that **L** showed a strong selectivity towards Hg^{2+} over other physiologically significant and environmentally metal ions.

Fluorescence titration of Hg^{2+} with probe **L**

To further investigate the properties of probe **L**, fluorescence titration experiments were conducted, as shown in Fig. 4. The emission of receptor **L** significantly enhanced at 582 nm with the level of Hg^{2+} increased, and the fluorescence emission was

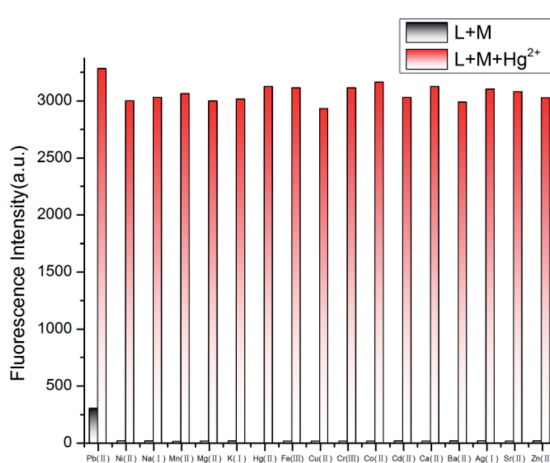


Fig. 3 The fluorescence intensity of **L** with Hg^{2+} in the presence of various competitive metal ions in $\text{CH}_3\text{OH}-\text{H}_2\text{O}$ (4 : 1, v/v, Tris-HCl buffer pH = 8.0).

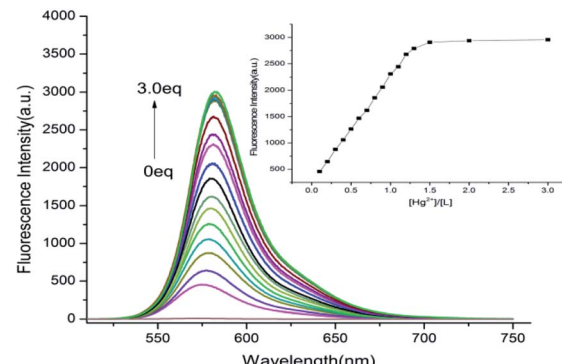


Fig. 4 Fluorescence emission spectra of probe **L** in the presence of various concentrations of Hg^{2+} (0–3 equiv.) in $\text{CH}_3\text{OH}-\text{H}_2\text{O}$ (4 : 1, v/v, Tris-HCl buffer pH = 8.0).

approximately increased to 55 fold when Hg^{2+} reached to 1.3×10^{-5} M.

The association constant (K) for the $\text{L}-\text{Hg}^{2+}$ complex was determined based on the Benesi–Hildebrand equation.²⁵ From Fig. S5(a),† K was determined to be $5.4 \times 10^4 \text{ M}^{-1}$. As demonstrated in Fig. S5(b),† working curves were established from titration data, which showed a reliable linear connection at the range of 0–13 μM for the concentration of Hg^{2+} . The LOD was $1.5 \times 10^{-9} \text{ M}$, which is lower than the limit quantity of Hg^{2+} ion in drinking water approved by the EPA.

Binding stoichiometry between probe **L** and Hg^{2+}

The stoichiometry of Hg^{2+} and probe **L** has been established by holding the quantity of the **L** and Hg^{2+} at 10 μM and adjusting the molar ratio of $[\text{Hg}^{2+}]/[\text{L} + \text{Hg}^{2+}]$ from 0 to 1. As showed in Fig. 5, the highest fluorescence value was obtained when the molar fraction approached 0.5. This phenomenon reveals a 1 : 1 stoichiometry for the Hg^{2+} and probe **L**. To further clarify the stoichiometry between probe **L** and Hg^{2+} , the MS analysis was carried out. When existence of 1.0 equiv. Hg^{2+} , a main peak at $m/z = 827.259[\text{L} + \text{Hg}^{2+} + \text{NO}_3^- + \text{H}^+]$ have been shown (Fig. S6†). It can be ascribed to the 1 : 1 $\text{L}-\text{Hg}^{2+}$ complex, which agree with

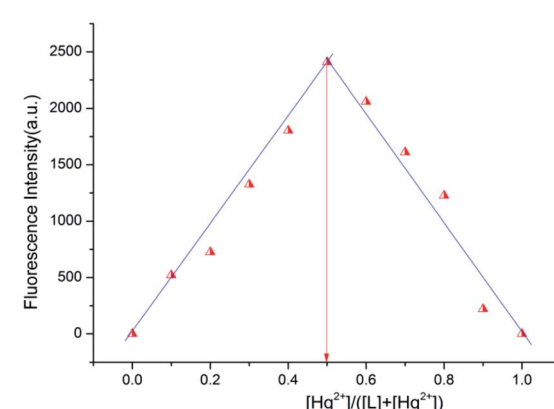


Fig. 5 Job's plot for determining the stoichiometry between **L** and Hg^{2+} ion in $\text{CH}_3\text{OH}-\text{H}_2\text{O}$ (4 : 1, v/v, Tris-HCl buffer pH = 8.0).



the results of the Job's plot. Simultaneously, a nitrate ion participates in the coordination of the Hg^{2+} .

The reversibility and regeneration of probe L toward Hg^{2+}

By introducing the EDTA aqueous solution to the $\text{L}-\text{Hg}^{2+}$ complex, the chemical reversibility and regeneration behaviors of **L** were examined. Probe **L** treated with Hg^{2+} showed a solid emission at 582 nm. After 20 equiv. EDTA was added, the fluorescence emission at 582 nm instantly dropped. The results show that EDTA is a better chelating agent than **L**. However, when the excessive Hg^{2+} (60 equiv.) were dropped to the above mixture, the emission at 582 nm appeared again. As described in Fig. 6, these findings show that the Hg^{2+} binding to **L** is chemically reversible and could be used for practical applications.

pH effect on free **L** and $\text{L}-\text{Hg}^{2+}$ complex

The impact of pH for the emission bands was investigated (Fig. 7). The emission intensity at 582 nm of receptor **L** decreased with the rise in the pH value when pH was less than 7.0. This phenomenon might be attributed to the spirolactam ring opening of probe **L**, which restored its conjugated structure as induced by the high concentration of H^+ .^{25,26} Once the pH was greater than 7.0, the emission of probe **L** disappeared immediately. It might be attributed to the presence of the spirolactam ring, which destroyed its conjugated structure for probe **L**. However, for the $\text{L}-\text{Hg}^{2+}$ complex, the emission at 582 nm gradually enhanced from the pH 3 to 5, and almost did not alter at a pH of 6–8, which were probably attributed to the restoration of the conjugated structure for the probe **L** induced by Hg^{2+} . These phenomena showed that probe **L** possesses a significant fluorescence emission toward Hg^{2+} in the range of 7.0–8.0, which could be potentially applied in some physiologically samples.

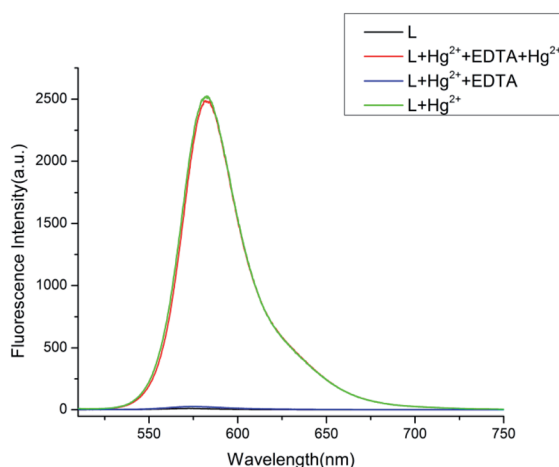


Fig. 6 Effect on fluorescence response of free **L** and $\text{L}-\text{Hg}^{2+}$ complex in $\text{CH}_3\text{OH}-\text{H}_2\text{O}$ (4 : 1, v/v, Tris–HCl buffer pH = 8.0) upon the addition of EDTA.

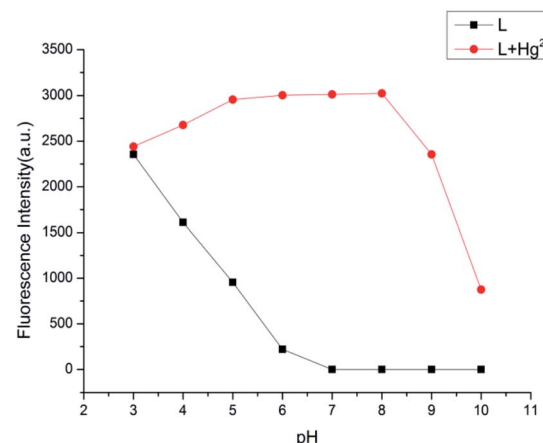


Fig. 7 Fluorescence intensity of probe **L** (10 μM) in the absence and presence of Hg^{2+} (10 equiv.) at different pH.

Complexation mechanism for $\text{L}-\text{Hg}^{2+}$

To understand the complexation behavior of receptor **L** with Hg^{2+} , ^1H NMR titration experiments were carried out in $\text{DMSO}-\text{d}_6$. The significant spectral differences upon the addition of Hg^{2+} are described in Fig. 8. In the presence of 1.0 equiv. Hg^{2+} , the protons of the imine (Hc') and thiophene ring (Ha', Hb') shifted downfield from 8.594 ppm to 8.672 ppm, 7.456 ppm to 7.467 ppm and 7.075 ppm to 7.087 ppm, respectively. This phenomenon suggested that the nitrogen atom in the imine moiety and the sulfur atom in the thiophene moiety might get involved in Hg^{2+} coordination. In addition, the proton of the benzene (Hd') was shifted downfield from 7.888 ppm to 7.903 ppm, and the protons in the benzene ($\text{e}', \text{f}',$ and g') were almost unaffected. This phenomenon indicated that the oxygen atom in the acyl hydrazone moiety might be involved in Hg^{2+} coordination, which is a significant factor for opening the spirolactam bond of the probe **L** and generating the xanthene moiety, which is in the conjugated state. To further clarify the sensing behavior of receptor **L** towards Hg^{2+} , IR analysis was carried out. Compared with free **L**, when 1.0 equiv. Hg^{2+} was added, the IR peak (Fig. S7†) for the $\text{C}=\text{O}$ amide bond of probe

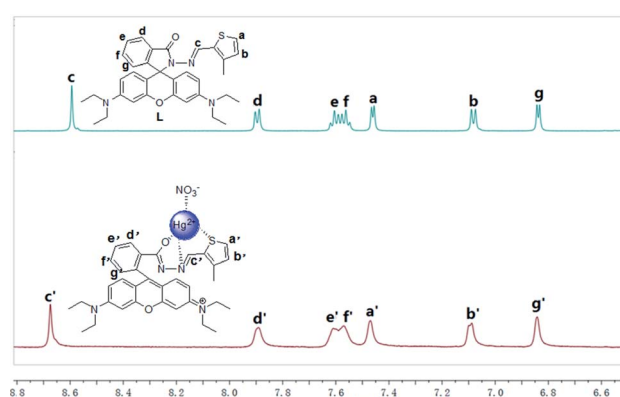


Fig. 8 ^1H NMR titration of the probe **L** in the presence of Hg^{2+} (1 equiv.).



L at 1684 cm^{-1} shifted to 1632 cm^{-1} , which was attributed to the oxygen atom of the acyl hydrazone moiety binding to Hg^{2+} ; moreover, Hg^{2+} induced the spirolactam ring opening of probe **L**.

For free probe **L**, the presence of the spirolactam ring destroys its conjugated structure. When excited with 520 nm light, the molecule has no fluorescence emission. Based on ^1H NMR titration, Job's plot, MS and IR analysis, a $1:1$ complex of **L** and Hg^{2+} was formed. Besides, the nitrogen atom in the imine moiety, the sulfur atom in the thiophene moiety, the oxygen atom in the acyl hydrazone moiety and a nitrate ion in the solution might get involved in Hg^{2+} coordination. While coordinating with the above atoms, Hg^{2+} induces the spirolactam ring opening of probe **L** to restore its conjugated structure. Once excited with 520 nm light, the L-Hg^{2+} complex has strong fluorescence emission. Protons can also induce the spirolactam ring opening of probe **L** when the pH is less than 7. The proposed sensing mechanism is shown in Scheme 2.

Cell imaging in living biological

By using MTT assay, the cytotoxicity of the solution, $\text{Hg}(\text{NO}_3)_2$, probe **L** and the L-Hg complex for MCF-7 cells were investigated following the reported method.²⁷ The results are shown in Fig. S8.† The viabilities of MCF-7 cells were more than 85% upon treatment with 5% $\text{CH}_3\text{OH}-\text{H}_2\text{O}$ (4 : 1) solution and $10\text{ }\mu\text{M}$ $\text{Hg}(\text{NO}_3)_2$ in $\text{CH}_3\text{OH}-\text{H}_2\text{O}$ (4 : 1) solution for 12 h, respectively. The results indicate that the solution of 5% $\text{CH}_3\text{OH}-\text{H}_2\text{O}$ (4 : 1) and $10\text{ }\mu\text{M}$ $\text{Hg}(\text{NO}_3)_2$ has little effect on the cell activity. When incubation with $10\text{--}70\text{ }\mu\text{M}$ probe **L** and L-Hg complex for 12 h respectively, cell viabilities were greater than 80% even at a concentration of $70\text{ }\mu\text{M}$, which indicated the satisfactory biocompatibility of the probe **L** and L-Hg^{2+} at $10\text{--}70\text{ }\mu\text{M}$. Besides, the determination of Hg^{2+} ions in MCF-7 cells was used to assess the potential biological application of **L**. The cells were cultured by the existed procedure.²⁸ As described in Fig. 9a, a red fluorescence was observed after the cells were treated with $10\text{ }\mu\text{M}$ Hg^{2+} ions. However, cells only supplementing $10\text{ }\mu\text{M}$

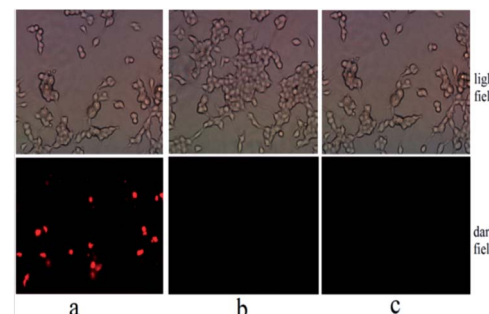


Fig. 9 Fluorescence images in MCF-7 cells. MCF-7 cells incubated with the $10\text{ }\mu\text{M}$ L-Hg^{2+} ions (a), MCF-7 cells incubated with the $10\text{ }\mu\text{M}$ probe **L** (b) and free MCF-7 cells (c).

probe **L** showed no fluorescence (Fig. 9b). These findings indicated that **L** may be used as a Hg^{2+} probe in biological systems.

Conclusions

In conclusion, a rhodamine-based probe **L** has been developed. The probe shows a "turn-on" response and clear colorimetric signal toward Hg^{2+} ions, which could be applied as an indicator. The spectral responses of **L** toward Hg^{2+} were robust over competitive ions. The binding mechanism of L-Hg^{2+} was studied via ^1H NMR titration, Job's plot, and MS and IR analyses, which show a $1:1$ complex of **L** and Hg^{2+} and the spirolactam bond was open when the Hg^{2+} ions were added. Furthermore, **L** can be utilized as a sensing material to image Hg^{2+} ions in MCF-7 cells.

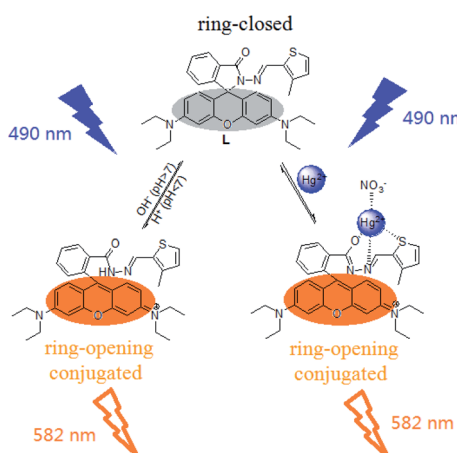
Conflicts of interest

There are no conflicts to declare.

Acknowledgements

This work was supported by the Scientific Research Project of Ordos Institute of Technology (Grant No. KYYB2021014).

Notes and references



Scheme 2 Proposed complexation mechanism of probe **L** and Hg^{2+} ions.

- 1 L. Feng, Y. Deng, X. Wang and M. Liu, *Sens. Actuators, B*, 2017, **245**, 441–447.
- 2 Y. Ding, Y. Pan and Y. Han, *Ind. Eng. Chem. Res.*, 2019, **58**, 7786–7793.
- 3 M. F. Wolfe, S. Schwarzbach and R. A. Sulaiman, *Environ. Toxicol. Chem.*, 1998, **17**, 146–160.
- 4 R. Singh, S. K. Rai, M. K. Tiwari, A. Mishra, A. K. Tewari, P. C. Mishra and R. K. Singh, *Chem. Phys. Lett.*, 2017, **676**, 39–45.
- 5 Q. Zhu, L. H. Liu, Y. P. Xing and X. H. Zhou, *J. Hazard. Mater.*, 2018, **355**, 50–55.
- 6 Q. Meng, C. He, W. Su, X. Zhang and C. Duan, *Sens. Actuators, B*, 2012, **174**, 312–317.



7 E. K. Silbergeld, I. A. Silva and J. F. Nyland, *Toxicol. Appl. Pharmacol.*, 2005, **207**, 282–292.

8 Q. Duan, H. Zhu, C. Liu, R. Yuan, Z. Fang, Z. Wang, P. Jia, Z. Li, W. Sheng and B. Zhu, *Analyst*, 2019, **144**, 1426–1432.

9 *Mercury Update Impact on Fish Advisories, EPA Fact Sheet EPA-823-F-01-011*, EPA Off., Washington, DC, 2001.

10 H. Cheng, C. Wu, L. Shen, J. Liu and Z. Xu, *Anal. Chim. Acta*, 2014, **828**, 9–16.

11 Y. Jia, Q. Mou, Y. Yu, Z. Shi, Y. Huang, S. Ni, R. Wang and Y. Gao, *Anal. Chem.*, 2019, **91**, 5217–5224.

12 O. Abollino, A. Giacomino, M. Malandrino, G. Piscionieri and E. Mentasti, *Electroanalysis*, 2010, **20**, 75–83.

13 D. Li, C. Y. Li, H. R. Qi, K. Y. Tan and Y. F. Li, *Sens. Actuators, B*, 2016, **223**, 705–712.

14 Y. Shiraishi, S. Sumiya, Y. Kohno and T. Hirai, *J. Org. Chem.*, 2008, **73**, 8571–8574.

15 X. Chen, Y. Xiang, Z. Li and A. Tong, *Anal. Chim. Acta*, 2008, **625**, 41–46.

16 H. N. Kim, W. X. Ren, J. S. Kim and J. Y. Yoon, *Chem. Soc. Rev.*, 2012, **41**, 3210–3244.

17 İ. Aydin, K. Ertekin, S. Oncuoglu and C. G. Hizliates, *Opt. Mater.*, 2021, **115**, 111030.

18 A. Kaya and J. Russ, *Coord. Chem.*, 2021, **47**, 903–908.

19 F. Liang, L. Xu, D. Jin, L. Dong, S. Lin, R. Huang, D. Song and P. Ma, *Luminescence*, 2022, **37**, 161–169.

20 H. Li, W. L. Sheng, L. Z. Wang, X. Meng, H. D. Duan and L. Q. Chi, *RSC Adv.*, 2021, **11**, 23597–23606.

21 Y. Li, Y. Zhang, M. Wang, D. Wang, K. Chen, P. Lin, Y. Ge, W. Liu and J. Wu, *J. Hazard. Mater.*, 2021, **415**, 125712.

22 Y. Cai, J. Wang, L. Niu, Y. Zhang, X. Liu, C. Liu, S. Yang, H. Qi and A. Liu, *Analyst*, 2021, **146**, 4630–4635.

23 S. Chemate and N. Sekar, *Sens. Actuators, B*, 2015, **220**, 1196–1204.

24 B. Muthuraj, R. Deshmukh, V. Trivedi and P. K. Iyer, *ACS Appl. Mater. Interfaces*, 2014, **6**, 6562–6569.

25 Y. Li, X. J. Wen, X. Y. Ding, X. Teng, X. H. Xiong and Y. Y. Liu, *Res. Chem. Intermed.*, 2022, **48**, 67–83.

26 K. Li, Y. Xiang, X. Wang, J. Li, R. Hu, A. Tong and B. Z. Tang, *J. Am. Chem. Soc.*, 2014, **136**, 1643–1649.

27 S. P. Wu, T. H. Wang and S. R. Liu, *Tetrahedron*, 2010, **66**, 9655–9660.

28 Q. Zhou, Z. M. Wu, X. H. Huang, F. F. Zhong and Q. Y. Cai, *Analyst*, 2015, **140**, 6720–6726.

